

# Direct measurement of the magnetic anisotropy field in Mn–Ga and Mn–Co–Ga Heusler films

Ciarán Fowley<sup>1</sup>, Siham Ouardi<sup>2</sup>, Takahide Kubota<sup>3</sup>,  
Yildirim Oguz<sup>1</sup>, Andreas Neudert<sup>1</sup>, Kilian Lenz<sup>1</sup>,  
Volker Sluka<sup>1</sup>, Jürgen Lindner<sup>1</sup>, Joseph M. Law<sup>4</sup>,  
Shigemi Mizukami<sup>3</sup>, Gerhard H. Fecher<sup>2</sup>, Claudia Felser<sup>2</sup>  
and Alina M. Deac<sup>1</sup>

<sup>1</sup> Institute of Ion Beam Physics and Materials Research, Helmholtz-Zentrum Dresden-Rossendorf, Bautzner Landstrasse 400, 01328 Dresden, Germany.

<sup>2</sup> Max-Planck-Institut für Chemische Physik fester Stoffe, Nöthnitzer Str. 40, 01187 Dresden.

<sup>3</sup> WPI-Advanced Institute for Materials Research (WPI-AIMR), Tohoku University, Sendai 980-8577, Japan

<sup>4</sup> High Magnetic Field Laboratory, Helmholtz-Zentrum Dresden-Rossendorf, Bautzner Landstrasse 400, 01328 Dresden, Germany.

E-mail: c.fowley@hzdr.de

## Abstract.

The static and dynamic magnetic properties of tetragonally distorted Mn–Ga based alloys were investigated. Static properties are determined in magnetic fields up to 6.5 T using SQUID magnetometry. For the pure Mn<sub>1.6</sub>Ga film, the saturation magnetisation is 0.36 MA/m and the coercivity is 0.29 T. Partial substitution of Mn by Co results in Mn<sub>2.6</sub>Co<sub>0.3</sub>Ga<sub>1.1</sub>. The saturation magnetisation of those films drops to 0.2 MA/m and the coercivity is increased to 1 T.

Time-resolved magneto-optical Kerr effect (TR-MOKE) is used to probe the high-frequency dynamics of Mn–Ga. The ferromagnetic resonance frequency extrapolated to zero-field is found to be 125 GHz with a Gilbert damping,  $\alpha$ , of 0.019. The anisotropy field is determined from both SQUID and TR-MOKE to be 4.5 T, corresponding to an effective anisotropy density of 0.81 MJ/m<sup>3</sup>.

Given the large anisotropy field of the Mn<sub>2.6</sub>Co<sub>0.3</sub>Ga<sub>1.1</sub> film, pulsed magnetic fields up to 60 T are used to determine the field strength required to saturate the film in the plane. For this, the extraordinary Hall effect was employed as a probe of the local magnetisation. By integrating the reconstructed in-plane magnetisation curve, the effective anisotropy energy density for Mn<sub>2.6</sub>Co<sub>0.3</sub>Ga<sub>1.1</sub> is determined to be 1.23 MJ/m<sup>3</sup>.

Submitted to: *J. Phys. D: Appl. Phys.*

## 1. Introduction

There has been a recent resurgence in research on Heusler alloys, in particular Mn-based ferrimagnetic compounds, for both magnetic storage and spin-transfer-torque applications due to the ability to widely tune the magnetic properties with varying composition [1–6]. The addition of Co to Mn–Ga allows the subtle tuning of magnetic properties, such as uniaxial anisotropy and saturation magnetisation [4]. These films can possess very high uniaxial anisotropy [7, 8]. They are promising for future rare-earth free permanent magnets [9]; highly stable magnetic recording elements scalable down to 10 nm bit size [3]; spin-polarised electrodes for tunnel magnetoresistance devices [10, 11]; as well as active elements in next generation spin-transfer torque devices such as THz-band spin transfer oscillators, due to their high ferromagnetic resonance frequencies and low Gilbert damping [7].

In these films, anisotropy fields of several tens of Tesla’s have been reported [3, 4, 6]. Combined with their low magnetisation, typically below 0.5 MA/m, traditional SQUID magnetometry and conventional ferromagnetic resonance (FMR) techniques are not so well suited for magnetic characterisation. For the majority of recent reports the anisotropy field is extrapolated from the intersection of the low field linear slope of the hard-axis magnetisation curve to the easy-axis saturation magnetisation. This intersection occurs at a field which is, in general, beyond the machine limit. For SQUID magnetometry this requires careful subtraction of the diamagnetic background signal [12]. It should also be pointed out that most studies to date have also been performed on thick samples, while more technologically relevant thinner films have shown reduced anisotropies [12]. Finally, measurement responses to standard SQUID- and FMR-based studies are also directly proportional to the total magnetic moment present. An alternative approach is to exploit electrical or optical detection techniques to characterise such materials. The direct measurement of the anisotropy field is especially required if there are additional, for example in-plane, anisotropy components to be considered in the material under investigation.

Time-resolved magneto-optical Kerr effect (TR-MOKE) has already been successfully used to characterise the high frequency dynamics of Mn–Ga thin films, showing precession frequencies between 200 GHz and 300 GHz [7]. The frequency of oscillation as a function of applied field can be fit with the Kittel formula. Such measurements therefore yield not only the ferromagnetic resonance (FMR) frequency and the Gilbert damping parameter,  $\alpha$ , but also the effective anisotropy field and energy density ( $\mu_0 H_k$  and  $K_{eff}$ , respectively). Provided the saturation magnetisation is known, the intrinsic uniaxial anisotropy  $K_u$  can be determined from  $K_{eff} = K_u - \frac{1}{2}\mu_0 M_S^2$ , where  $\frac{1}{2}\mu_0 M_S^2$  represents the demagnetising energy of an extended thin-film.

The extraordinary Hall effect (EHE) is a very useful characterisation tool for these perpendicularly magnetised materials [13]. When a current is applied along a certain direction in a film, the transverse resistivity ( $\rho_{xy}$ ) is directly proportional to the out-of-plane magnetisation component ( $M_z$ ) via the extraordinary Hall coefficient,  $R_{EHE}$  [14]. For perpendicular anisotropy materials, if we apply an external field along the easy axis of the film and switch the magnetisation, and therefore  $\rho_{xy}$ , we will obtain an electrical equivalent of the magnetic hysteresis loop. Similarly, when the field is applied along the hard axis, the saturation of the magnetisation can be seen as a gradual change and saturation of  $\rho_{xy}$ . From the hard axis data, the anisotropy field,  $\mu_0 H_k$ , can be determined. EHE allows for characterisation of these high-anisotropy

films beyond what is normally accessible from standard magnetometry for several reasons: firstly, it is a transport technique and not a magnetometry technique, which means it can be used to measure the magnetic response of volumes of material and/or patterned structures which would be otherwise undetectable; secondly, an inherent advantage is that  $\rho_{xy}$  exhibits an inverse thickness dependence meaning that the EHE signal is larger for thinner films; thirdly,  $R_{EHE}$  in ferromagnetic materials is large meaning that even though  $M_S$  may be low,  $\rho_{xy}$  can be high. These advantages make EHE an ideal probe of the magnetisation at lower thickness and/or confined geometry.

In the search for materials with higher perpendicular anisotropy and lower saturation magnetisation for spin-transfer-torque applications, alternative characterisation techniques, such as those outlined above, will become increasingly more important. To exemplify this, we investigate  $L1_0$   $Mn_{1.6}Ga$  (Mn–Ga) and  $Mn_{2.6}Co_{0.3}Ga_{1.1}$  (Mn–Co–Ga) using TR-MOKE and EHE in high magnetic fields. Both materials possess high uniaxial anisotropy. In particular, the chosen composition of Mn–Co–Ga has been shown to exhibit very low saturation magnetisation while retaining high anisotropy [4]. They therefore represent ideal samples for determining the usefulness of the techniques as the properties are favourable for applications while at the same time may prove difficult to determine with more traditional methods, especially at reduced thicknesses [13]. We show that, in particular, EHE at high magnetic fields is an ideal method for determining the anisotropy field of such Heusler systems.

## 2. Experimental details

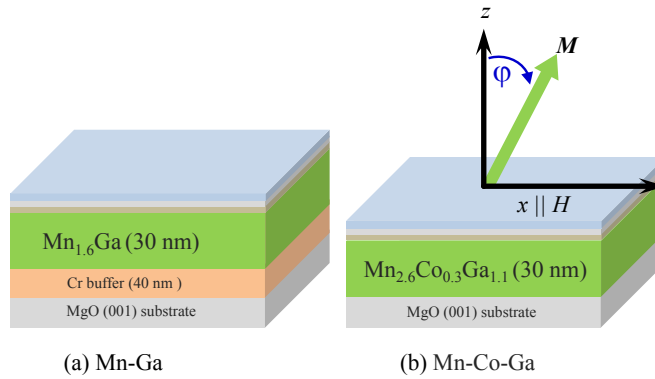


**Figure 1.** Sketch of the  $Mn_{1.6}Ga$  (a) and  $Mn_{2.6}Co_{0.3}Ga_{1.1}$  (b) film stacks. The topmost layers are Mg, MgO, and  $AlO_x$  to protect the sample from oxidation (see text for thicknesses).

Tetragonal Mn–Ga and Mn–Co–Ga thin films were grown by ultra-high-vacuum sputtering on single crystal MgO(001) substrates. Specific details on sample fabrication and growth conditions can be found in Reference [4]. The stacking structures of the multi-layered films are:

MgO(100) substrate / Cr(40) /  $Mn_{1.6}Ga$ (30) / Mg(0.4) / MgO(2.0) /  $AlO_x$ (1.3) and  
 MgO(100) substrate /  $Mn_{2.6}Co_{0.3}Ga_{1.1}$ (30) / Mg(0.4) / MgO(2.0) /  $AlO_x$ (1.3)

as sketched in Figures 1(a) and (b), respectively. The thickness, in nm, is appended

in brackets after each material. The topmost three layers were added to simulate a tunnelling barrier and to protect the sample from oxidation.

Low-field magnetization data were obtained by magnetic field dependent magnetisation measurements at 300 K, up to an applied external field of 6.5 T using conventional SQUID magnetometry. TR-MOKE was used to characterise the high frequency dynamic properties of the Mn<sub>1.6</sub>Ga film. An 800 nm pump beam with a power of 31.2 mW at the sample, leads to ultra-fast demagnetisation of the sample. The laser pulses were 100 fs in length with a repetition rate of 5.2 MHz. A fixed-delay probe beam of 400 nm, with a power of 105  $\mu$ W at the sample is then used to probe the excited dynamics via lock-in detection. The diameter of the spot sizes of the pump and probe beams were 17  $\mu$ m and 5  $\mu$ m, respectively. The pump and probe fluences, calculated from the incident power, beam diameter and repetition frequency 1.32 mJ/cm<sup>2</sup> and 0.05 mJ/cm<sup>2</sup>, respectively. Time resolution is obtained by a variable delay line on the pump beam which allows for the measurement of changes in magnetisation both before and after the demagnetisation process.

EHE was measured initially using a DC current of 1 mA at room temperature in a magnetotransport set-up capable of applying fields up to 1.6 T. Subsequent EHE measurements were performed in a cryostat at 77 K using pulsed magnetic fields at the High Magnetic Field Laboratory located in the Helmholtz-Zentrum Dresden-Rossendorf. The pulsed magnet which was used had a rise time of 7 ms, a fall time of 24 ms and a maximum field of approximately 60 T. An sinusoidal AC current of 1 mA was applied to the sample with a frequency of 47.62 kHz. The transverse voltage was measured during the magnetic field pulse and the signal was locked-in post experiment via a digital lock-in program.

EHE scans along the easy and hard axes, in combination with the evaluated  $M_S$  from SQUID, allows for the direct determination of the anisotropy field,  $\mu_0 H_k$ , as well as the effective anisotropy energy,  $K_{eff}$ , by integration of normalised magnetisation loops.

### 3. Magnetic properties

The initial magnetic characterisation of the thin films using SQUID is shown in Figure 2. The pure Mn–Ga film – shown in figure 2 a) – exhibits sharp hysteretic switching when the field is applied in the out-of-plane direction (closed red circles) with a coercive field,  $\mu_0 H_c$ , of 290 mT. The data show clearly that the easy axis is along the film normal. A small in-plane component appears in the hard axis measurements consistent with an intrinsic canted moment on the 2b Mn sub-lattice [6]. The saturation magnetisation,  $M_S$ , is 0.36 MA/m. In-plane (open black squares) magnetisation measurements give an anisotropy field,  $\mu_0 H_K$ , of 4.5 T, which was also verified by vibrating sample magnetometry (VSM) up to 14 T (not shown here). These values correspond to an anisotropy energy density  $K_{eff}$  of 0.81 MJ/m<sup>3</sup>.

The addition of Co into Mn–Ga, shown in figure 2 b), leads to a reduction of the  $M_S$  to 0.2 MA/m and an accompanied increase of  $\mu_0 H_c$  to 928 mT. The anisotropy field is also increased to a value beyond 5 T. For the in-plane curve, the same diamagnetic background as in the out-of-plane measurement was subtracted from the raw data, however as can be seen from the data, an accurate determination of the anisotropy field is not possible. VSM magnetometry up to 14 T was not able to confirm the anisotropy field due to a low magnetisation signal (not shown). We note that, as opposed to the Mn–Ga film we have a soft magnetic component in both

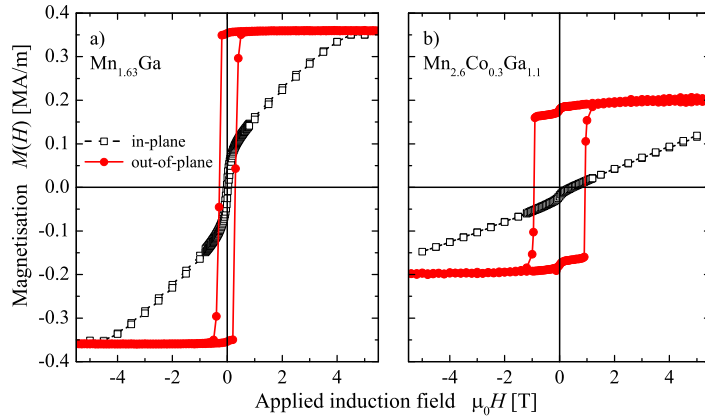


**Figure 2.** Static magnetic properties at 300 K for a) Mn–Ga and b) Mn–Co–Ga films. Both films exhibit strong perpendicular magnetic anisotropy, with approximately square hysteresis loops and  $M_r/M_S \approx 1$ . The addition of Co results in a drop of the magnetisation accompanied by an increase in both the coercive field and the anisotropy field (increased beyond 5 T).

the in-plane and out-of-plane magnetisation curves indicating that we do not have the same canted moment as in the pure film. Rather, the data seem to indicate a segregated phase lacking any anisotropy axis. This could be initially attributed to Co clusters in the film or a lack of full epitaxial growth due to the lack of seed layer.

The  $M(H)$  hysteresis curves of both materials are nearly rectangular. The energy product is thus given by  $E = B_r \times H_c$ , where  $B_r$  and  $H_c$  are the remanence and the coercive field, respectively. The out-of-plane energy products are  $104 \text{ kJ/m}^3$  for  $\text{Mn}_{1.6}\text{Ga}$  and  $165 \text{ kJ/m}^3$  for  $\text{Mn}_{2.6}\text{Co}_{0.3}\text{Ga}_{1.1}$ . The addition of Co leads to a reduction of the maximum energy product,  $BH_{\text{max}}$ , from about 40 to  $10 \text{ kJ/m}^3$ . The values of the energy product and  $BH_{\text{max}}$  for  $\text{Mn}_{2.6}\text{Co}_{0.3}\text{Ga}_{1.1}$  are of the same order as bulk  $\text{Mn}_3\text{Ga}$  (cf. Reference [15]).

Figure 3 shows the EHE curves obtained from  $5 \text{ mm} \times 5 \text{ mm}$  square films measured in the van der Pauw geometry. For both films, the coercivity is identical to that obtained from SQUID measurements. The magnitude of  $\rho_{xy}$  for Mn–Ga is much lower than that obtained for the Mn–Co–Ga film. Although the underlying Cr layer is responsible for current shunting, it is anyway expected that pure Mn–Ga films show a lower Hall signal with improving crystal quality [13]. It can be seen that the EHE curve for the Co–Mn–Ga films does not trace out the additional change in magnetisation close to zero field as seen in figure 2 (b). As has been calculated for Co-doped Mn–Ga films, Co substitutes Mn randomly at both the  $2b$  and  $4d$  positions, fills the minority band at  $E_F$  and leads to the localisation of electrons in the minority band [16]. Assuming that the soft magnetic component seen in SQUID is related solely to Co substitution, it is likely that, due to the increased electron localisation, the contribution of Co to the magnetotransport is diminished, therefore the same soft phase is not reproduced in the EHE measurement.

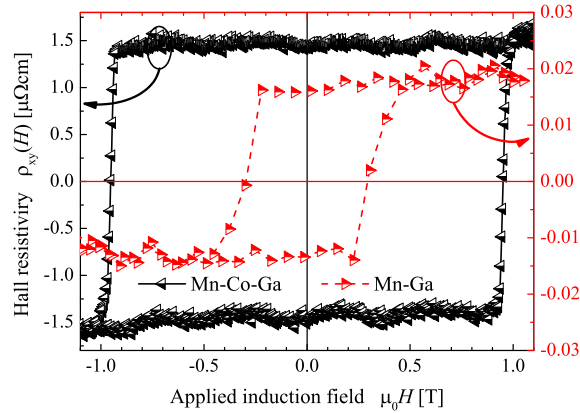


**Figure 3.** Extraordinary Hall effect data measured at room temperature for Mn-Ga and Mn-Co-Ga films. The coercive fields match exactly with those obtained from SQUID in figure 2. Note that the magnitudes of  $\rho_{xy}$  for the two films differ by about two orders of magnitude.

#### 4. Time-resolved MOKE

TR-MOKE was used to evaluate the effective anisotropy of the Mn-Ga film. A magnetic field of 0.65 to 1.3 T was applied at  $60^\circ$  to the film normal in order to cant the magnetisation away from the easy axis. This provides a projection of the precession along the film normal which is then measured in the polar MOKE geometry.

Figure 4 a) shows several TR-MOKE spectra at different applied magnetic fields as well as the fitted curves from which the frequency and damping are extracted. It can be seen in this figure that the magnetisation, after the initial demagnetisation pulse at  $t = 0$ , oscillates around the effective field direction leading to a characteristic oscillation of the optical signal. The ferromagnetic resonance frequency ( $f_{res}$ ) and the Gilbert damping parameter ( $\alpha$ ) are extracted by fitting these curves with the Kittel formula for the uniform mode.  $f_{res}$  and  $\alpha$  are plotted in figure 4 b) and c), respectively. The precession frequency was found to vary between 136 GHz and 142 GHz in the aforementioned field range. The slope of the fitted line in figure 4 b) is 11.4 GHz/T. The Gilbert damping parameter is found to be roughly independent of the applied field and has an average value of 0.019. By fitting  $f_{res}$  versus applied field the effective anisotropy of the film can also be evaluated. The extracted value of value of 4.5 T obtained from fitting is in excellent agreement with the value obtained from the SQUID measurement. This, combined with a single peak in the FFT of the spectra, indicate that the uniform precession mode is the dominant contribution to the TR-MOKE signal. The values of  $f_{res}$  and  $\alpha$  obtained for this film also compare well to those in the literature [7]. Furthermore, they demonstrate the potential use of high anisotropy alloys as microwave oscillators beyond 100 GHz.

#### 5. High-field EHE

As previously mentioned, the anisotropy field of the Mn-Co-Ga film is beyond the accessible range of both the SQUID and the VSM (maximum field of 6.5 T and 14 T, respectively). For the Mn-Co-Ga sample, it was also not possible to obtain

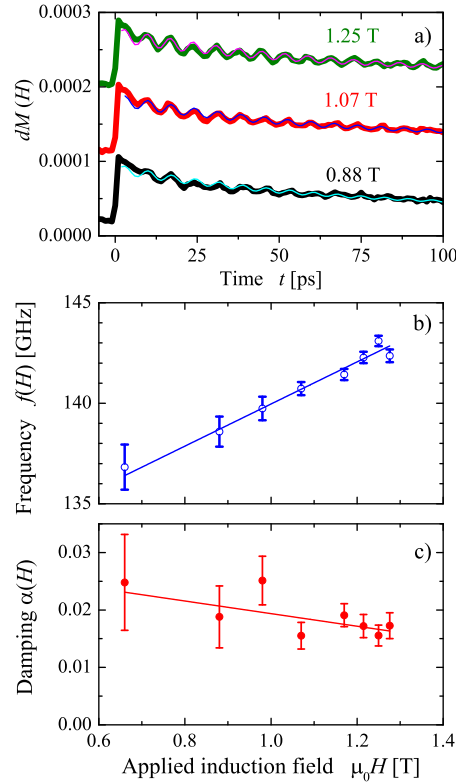


**Figure 4.** a) TR-MOKE spectra (bold lines) together with fitting curves (thin lines) for the Mn–Ga film at various fields applied  $60^\circ$  to the film normal. b) Frequency and c) damping as a function of applied field strength. Lines in b) and c) result from linear fits.

any ferromagnetic resonance data from the TR-MOKE which is most likely due to the inability to obtain a large enough canting angle for polar MOKE detection. We therefore determine the anisotropy field using EHE as a detection method.

Figure 5 a) shows the EHE curves for both in-plane and out-of-plane applied fields up to 35 T. The EHE response with the field applied out-of-plane (open red triangles) is, again, identical to that obtained from SQUID measurements with sharp switching of the magnetisation visible at approximately 1 T. When the magnetic field is applied in the plane of the sample (closed black triangles) the magnetisation gradually cants to the plane of the film. Since the EHE signal is only sensitive to the out-of-plane component of magnetisation,  $M_z$ , the in-plane component of the magnetisation,  $M_x$ , must be reconstructed. This is achieved using the transform,  $\sin(\cos^{-1}(M_z))$  because the projection of the magnetisation along  $z$  is simply  $\cos(\phi)$ , where  $\phi$  is the angle of the magnetisation to the film normal (see Figure 5 b) inset and Figure 1b)).

Figure 5 b) shows the both the  $M_z$  component (open red circles), the reconstructed in-plane  $M_x$  component (open black squares), and the canting angle,  $\phi$  (blue dashed line). Here, both  $M_x$  and  $M_z$  have been normalised to the maximum. It can be seen from the figure that the  $M_x$  component is almost totally saturated at 12 T and is completely saturated at 18 T. The anisotropy energy is obtained by evaluating

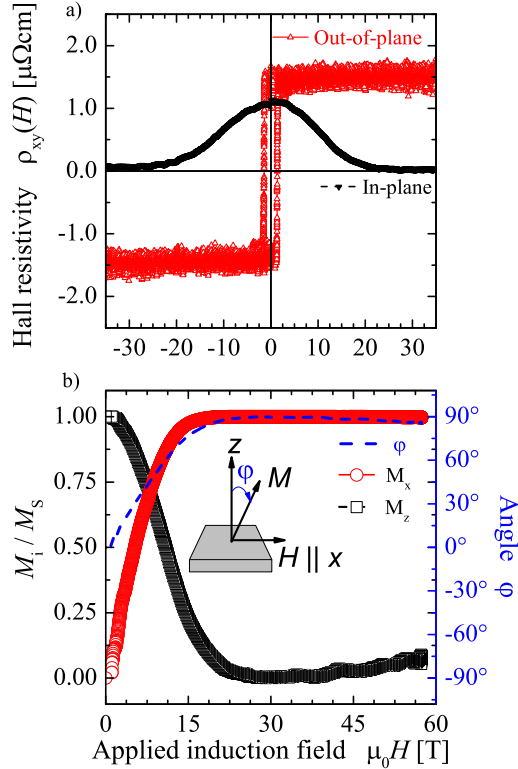


**Figure 5.** a) EHE response of the Mn–Co–Ga film, measured with in-plane and out-of-plane fields up to 35 T. b) reconstructed in-plane magnetisation curve ( $M_x/M_S$ ) and angle of magnetisation ( $\phi$ ) as a function of applied field up to approximately 60 T.

the integral  $\int_0^{M_S} \mu_0 H_x \cdot dM_x$  between zero and saturation, i.e the area enclosed by the reconstructed  $M_x$  curve and the  $y$ -axis, and multiplying this by  $M_S$ . Beyond saturation the  $M_z$  component of magnetisation begins to increase. This is attributed to a small offset between the applied field direction and the film plane. Although the change is rather large in  $M_z$  it corresponds to a misalignment of less than  $5^\circ$ .

From the integration of the area between the reconstructed in-plane and out-of-plane loops a value of  $K_{eff}$  of  $1.23 \text{ MJ/m}^3$  is obtained. Although the TR-MOKE results were inconclusive with the Mn–Co–Ga sample, the given value of anisotropy field and saturation magnetization yield precession frequencies of order 350 GHz.

## 6. Conclusion

We have investigated static and dynamic magnetic properties of  $\text{Mn}_{1.6}\text{Ga}$  and  $\text{Mn}_{2.6}\text{Co}_{0.3}\text{Ga}_{1.1}$  films. As expected, these materials possess a low saturation magnetisation and high uniaxial anisotropy, usually beyond the accessible field range available in typical SQUID magnetometers. Consequently, standard magnetometry was combined with both time resolved magneto-optical Kerr effect and extraordinary Hall effect in high magnetic fields to ascertain exact values for the magnetic anisotropy

of both types of thin films.

For the pure  $\text{Mn}_{1.6}\text{Ga}$  alloy, we find a magnetic anisotropy energy of  $0.81 \text{ MJ/m}^3$ , with a saturation magnetisation of  $0.36 \text{ MA/m}$ . The partial substitution of Mn by Co increases the effective anisotropy energy to  $1.23 \text{ MJ/m}^3$  and decreases the saturation magnetisation of  $0.2 \text{ MA/m}$ .

Time-resolved magneto-optical Kerr effect and extraordinary Hall effect were utilised to directly probe the anisotropy fields of both materials. The measured values are  $4.5 \text{ T}$  and  $18 \text{ T}$  for  $\text{Mn}_{1.6}\text{Ga}$  and  $\text{Mn}_{2.6}\text{Co}_{0.3}\text{Ga}_{1.1}$ , respectively.

In summary, we have shown that both time-resolved magneto-optical Kerr-effect and the extraordinary Hall effect in high magnetic fields are extremely useful techniques in determining the anisotropy energy for materials which cannot be saturated in standard magnetometers such as SQUID. Such indirect techniques can be readily applied to technologically relevant high anisotropy materials for spin-transfer-torque applications.

### Acknowledgments

C.F. would like to acknowledge Dr. Marc Uhlarz for fruitful discussions. Financial support by DfG-JST is gratefully acknowledged (projects P 1.3-A and P 2.1-A of the Research Unit FOR 1464 *ASPIMATT*). Part of this work was funded by EuroMagNET under EU contract no. 228043.

- [1] B. Balke, G. H. Fecher, J. Winterlik, C. Felser, M. C. M. Alves, F. Bernardi, and J. Morais. *Phys. Rev. B*, 77:054406, 2008.
- [2] V. Alijani, J. Winterlik, G. H. Fecher, and C. Felser. *Appl. Phys. Lett.*, 99:222510, 2011.
- [3] H. Kurt, K. Rode, M. Venkatesan, P. Stamenov, and J. M. D. Coey. *Phys. Rev. B*, 83(2):020405, 2011.
- [4] S. Ouardi, T. Kubota, G. H. Fecher, R. Stinshoff, S. Mizukami, T. Miyazaki, E. Ikenaga, and C. Felser. *Appl. Phys. Lett.*, 101(24):242406, 2012.
- [5] T. Kubota, S. Ouardi, S. Mizukami, G. H. Fecher, C. Felser, Y. Ando, and T. Miyazaki. *J. Appl. Phys.*, 113:17C723, 2013.
- [6] K. Rode, N. Baadji, D. Betto, Y.-C. Lau, H. Kurt, M. Venkatesan, P. Stamenov, S. Sanvito, and J. M. D. Coey. *Phys. Rev. B*, 87:184429, 2013.
- [7] S. Mizukami, F. Wu, A. Sakuma, J. Walowski, D. Watanabe, T. Kubota, X. Zhang, H. Naganuma, M. Oogane, Y. Ando, and T. Miyazaki. *Phys. Rev. Lett.*, 106(11):117201, 2011.
- [8] H. Kurt, K. Rode, P. Stamenov, M. Venkatesan, Yong-Chang Lau, E. Fonda, and J. M. D. Coey. *Phys. Rev. Lett.*, 112:027201, 2014.
- [9] J. M. D. Coey. *J. Phys.: Condens. Matter*, 26:064211, 2014.
- [10] T. Kubota, Y. Miura, D. Watanabe, S. Mizukami, F. Wu, H. Naganuma, X. Zhang, M. Oogane, M. Shirai, Y. Ando, and T. Miyazaki. *Appl. Phys. Express*, 4:043002, 2011.
- [11] Q. L. Ma, T. Kubota, S. Mizukami, X. M. Zhang, H. Naganuma, M. Oogane, Y. Ando, and T. Miyazaki. *Appl. Phys. Lett.*, 101(3):032402, 2012.
- [12] A. Köhler, I. Knez, D. Ebke, C. Felser, and S. S. P. Parkin. *Appl. Phys. Lett.*, 103(16):162406, 2013.
- [13] M. Glas, D. Ebke, I. M. Imort, P. Thomas, and G. Reiss. *J. Magn. Magn. Mater*, 333(0):134, 2013.
- [14] N. Nagaosa, J. Sinova, S. Onoda, A. H. MacDonald, and N. P. Ong. *Rev. Mod. Phys.*, 82(2):1539, 2010.
- [15] J. Winterlik, B. , Balke, G. H. Fecher, and C. Felser. *Appl. Phys. Lett.*, 90:152504, 2007.
- [16] A. Chadov, J. Kiss, and C. Felser. *Adv. Func. Mat.*, 23:832, 2013.